Exchange interactions, Jahn-Teller coupling, and multipole orders in pseudospin one-half $5d^2$ Mott insulators

Giniyat Khaliullin [1,*] Derek Churchill [2], P. Peter Stavropoulos [2], and Hae-Young Kee [2,3,†]

[1]*Max Planck Institute for Solid State Research, Heisenbergstrasse 1, D-70569 Stuttgart, Germany*
[2]*Department of Physics, University of Toronto, Ontario, Canada M5S 1A7*
[3]*Canadian Institute for Advanced Research, CIFAR Program in Quantum Materials, Toronto, Ontario, Canada M5G 1M1*

We develop a microscopic theory of multipole interactions and orderings in $5d^2$ transition metal ion compounds. In a cubic environment, the ground state of $5d^2$ ions is a non-Kramers E_g doublet, which is nonmagnetic but hosts quadrupole and octupole moments. We derive low-energy pseudospin one-half Hamiltonians describing various spin-orbital exchange processes between these ions. Direct overlap of the t_{2g} orbitals results in bond-dependent pseudospin interactions similar to those for e_g orbitals in manganites, except for different orientations of the pseudospin easy axes. On the other hand, the superexchange process, where two different t_{2g} orbitals communicate via oxygen ions, generates new types of pairwise interactions. In perovskites with 180° bonding, we find nearly equal mixture of Heisenberg and e_g orbital compass-type couplings. The 90° superexchange in compounds with edge-shared octahedra is most unusual: Despite highly anisotropic shapes of the E_g wave functions, the pseudospin interactions have no bond dependence. We consider the E_g pseudospin models on various lattices and obtain their ground state properties using analytical and numerical methods. On the honeycomb lattice, we observe a duality with the extended Kitaev model, and use it to uncover a critical point where the quadrupole and octupole states are exactly degenerate. On the triangular lattice, an exotic pseudospin state, corresponding to the coherent superposition of vortex-type quadrupole and ferri-type octupole orders, is realized due to geometrical frustration. This state breaks both spatial and time-reversal symmetries, but possesses no dipolar magnetism. We also consider Jahn-Teller coupling effects and lattice mediated interactions between E_g pseudospins, and find that they support quadrupole order. Possible implications of the results for recent experiments on double perovskite osmates are discussed, including effects of local distortions on the pseudospin wave functions and interactions.

I. INTRODUCTION

As a hallmark of strong correlations, the spin-orbital multiplet structure of ions is largely preserved in transition metal (TM) compounds. At low temperatures, the spin and orbital degeneracy of these multiplet levels has to be lifted one way or another. Apart from exotic means of the entropy quenching such as formation of quantum spin and orbital liquids, this is typically done by long-range ordering of spins and orbitals, or their composites, through symmetry breaking phase transitions.

Broadly speaking, the interactions driving these phase transitions have three different microscopic origins: (a) Jahn-Teller orbital-lattice coupling, (b) Kugel-Khomskii type

spin-orbital exchange, and (c) relativistic spin-orbit coupling (SOC). Depending on the multiplet structure of constituent ions and the nature of chemical bonds in a crystal, the interplay between these couplings may take various forms, resulting in rich spin-orbital physics in TM compounds.

Lifting the orbital degeneracy via a cooperative Jahn-Teller (JT) structural transition is most common in e_g-orbital systems like manganites. At this transition, the orbitals are (self)trapped by static lattice distortions. The JT driven orbital order is essentially independent of spins and happens well before magnetic ordering. In this picture, the low-energy physics is given by "spin-only" Hamiltonians, with the exchange parameters dictated by the Goodenough-Kanamori rules [1,2].

In t_{2g}-orbital systems with relatively weak JT coupling, the spin S and orbital L degrees of freedom are no longer separated [3]. They may instead develop joint dynamics driven by the spin-orbital exchange interactions, as well as by intraionic SOC, which unifies the two sectors by forming total angular momentum $J = S + L$. The latter root to the "spin-orbital-entangled" physics is especially relevant to $4d$ and $5d$ electron compounds.

In the strong SOC limit, the JT orbital-lattice coupling and Kugel-Khomskii exchange interactions have to be

*g.khaliullin@fkf.mpg.de
†hykee@physics.utoronto.ca

reformulated in terms of total angular momentum J of the lowest multiplet level, as is usually done in $4f$ electron systems. This leads to a number of important consequences. First, the JT-orbital order is "converted" into quadrupole order of J moments, involving also the spin sector, which was initially "blind" to JT physics. Effective JT coupling is typically reduced, due to a partial suppression of the initial orbital degeneracy. Second, exchange interactions between effective J moments ("pseudospins") may become highly anisotropic and bond-directional; this is due to the nonspherical shape of the spin-orbit entangled wave functions. Third, pseudospin states may carry not only dipole or quadrupole moments, but also higher-rank multipoles such as a magnetic octupole.

The physical content of pseudospin wave functions is decided by a filling factor n of d-orbital levels. In combination with the lattice and chemical bonding geometry in a given material, this leads to a variety of nontrivial interactions and ground states among different d^n compounds. This includes a possible realization of Kitaev spin-liquids, excitonic magnetism, and multipole orders (for a recent review, see Ref. [4]).

In this paper, we focus on spin-orbital physics in compounds based on d^2 ions. The d^2 configuration with two-electron spin $S = 1$ and effective orbital moment $L = 1$ is special, because its total angular momentum $J = 2$ is isomorphic (in terms of the degeneracy and symmetry properties) to a single d-electron orbital moment $l = 2$ [4]. This formal analogy has interesting implications for the symmetry and physical properties of d^2 ions. Namely, in a cubic environment, a $J = 2$ level has to split into E_g doublet and T_{2g} triplet levels by an energy Δ_c [see Fig. 1(a)], just like the d-electron $l = 2$ level splits into e_g and t_{2g}-orbital levels by a cubic crystal field [5]. While the T_{2g} triplet hosts an effective angular momentum $\widetilde{J} = 1$ (with a familiar relation $\widetilde{J} = -J$) [6], the non-Kramers E_g doublet is similar to an e_g-orbital doublet, which carriers no dipole but the quadrupole and octupole moments instead [7–10]. This implies that d^2 ions with non-Kramers E_g ground states may show high-rank multipole orders, similar to rare-earth f^2 non-Kramers Γ_3 ions [11]. We note that while the non-Kramers doublets $d^2(E_g)$, $d^1(e_g)$, and $f^2(\Gamma_3)$ share the same symmetry, their "internal" structure and hence physical properties (e.g., exchange interactions and orderings) are different, as we will see below. As the cubic splitting Δ_c increases with the strength of SOC, the spin-orbit entangled E_g multipoles are most protected and realized in materials based on heavy, especially $5d^2$, transition-metal ions.

Experimentally, a single phase transition around 30–50 K is observed in $5d^2$ double perovskite (DP) compounds [12–15]. This is very different from $5d^1$ Kramers ion DPs, which show two separate transitions [16–19], corresponding to quadrupole (structural) and dipole orders of $J = 3/2$ states [20,21]. Having a single transition is natural for pseudospin-1/2 doublet systems, and this clearly points to the E_g doublet physics in $5d^2$ DPs. However, the precise nature of this transition is not yet fully established. The structural changes at this transition, if any, are found to be below 0.1% [12]. While no magnetic Bragg peaks were seen in neutron diffraction data, time-reversal (TR) symmetry breaking is detected by muon spin relaxation. To reconcile these observations, a ferro-type octupolar order of the E_g doublets has been proposed [12,22,23].
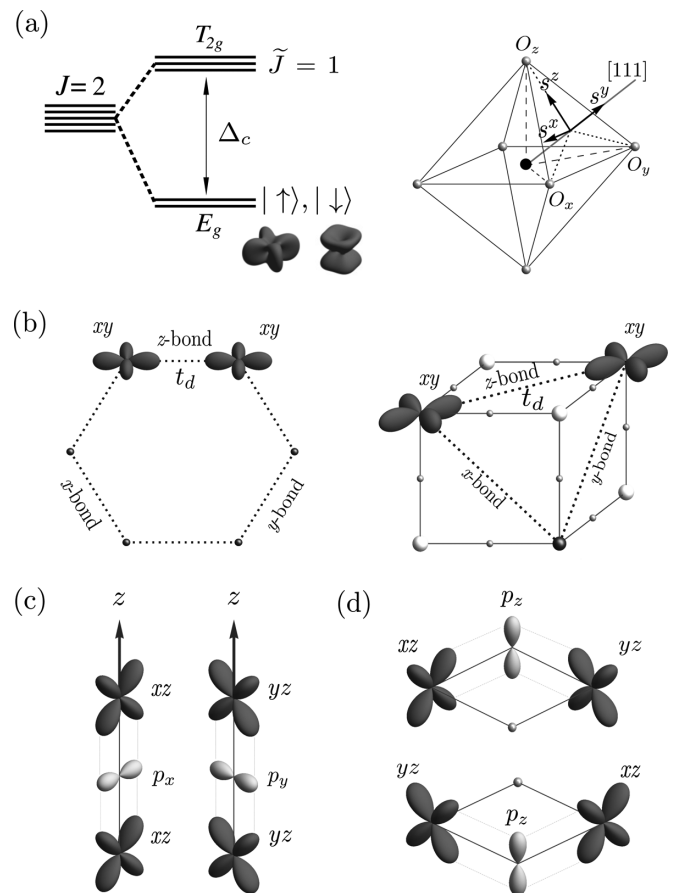

FIG. 1. (a) Cubic splitting Δ_c of the $J = 2$ level, and the spatial shapes of E_g-doublet wave functions (see also Fig. 2 of Ref. [4]). Right panel shows the pseudospin (s^x, s^y, s^z) coordinate axes with respect to oxygen octahedra. (b) Direct hopping between xy orbitals in honeycomb (left) and double perovskite (right) lattices, resulting in bond-dependent pseudospin τ interactions Eq. (10) between spin-orbit entangled E_g states. (c) Two-orbital superexchange via $180°$ Me-O-Me bonding geometry. Hopping is orbital conserving: $xz \leftrightarrow xz$ and $yz \leftrightarrow yz$. This process results in pseudospin interactions Eq. (13), comprising isotropic Heisenberg and bond-dependent compass-type couplings. (d) Two-orbital superexchange via $90°$ bonding geometry. Hopping interchanges the orbital labels: $xz \leftrightarrow yz$. This process leads to the interactions Eq. (15), which are anisotropic in pseudospin space but have no bond dependence.

The octupole is a third-rank magnetic multipole, which carries no dipole moment, and its long-range order is observed in rare-earth compounds (see Ref. [11] for a review of multipole orders). The possibility of octupolar order in d-electron systems is intriguing. It is actually quite unexpected because an E_g doublet is subject to JT physics: its partners have different charge density shapes (planar and elongated), see Fig. 1(a). Therefore, a conventional quadrupole order like in e_g-orbital systems [2] is the most natural instability to expect in the first place. To realize the octupolar order, exchange interactions between the octupole moments must be strong enough to overcome the quadrupolar interactions contributed by the Kugel-Khomskii exchange and orbital-lattice JT couplings.

Early theoretical work [24] on d^2 DP systems with strong SOC assumed that cubic splitting of the $J = 2$ level Δ_c is

smaller than the exchange couplings and therefore neglected it. The obtained phase diagram contains dipolar and quadrupolar ordered states. Here we develop a theory of d^2 electron systems starting from the opposite limit, i.e., when cubic splitting Δ_c is large and the E_g doublet is well separated from the virtual T_{2g} states, as actually seen in experiment [12]. Having in mind $5d^2$ materials other than double perovskite compounds, we keep the discussion as general as possible, considering various spin-orbital exchange processes typical in TM oxides. The resulting E_g-doublet interactions are represented in terms of pseudospin one-half Hamiltonians. In most cases, the interactions are dominated by quadrupolar couplings. In a 90° exchange geometry however, the quadrupole and octupole channels are equally present, and effective interactions on a single bond can be written in a Heisenberg form with no preference for either of these two channels. The resulting multipole orders of E_g doublets in different lattices are considered. On a honeycomb lattice, we show that the E_g-pseudospin model can be mapped to the extended Kitaev model, thereby uncovering a hidden SU(2) symmetry point that separates quadrupole and octupole orders. The pseudospins on a geometrically frustrated triangular lattice show more complex phase behavior, including a coherent mixture of different rank (quadrupole and octupole) orders in the ground state. The order parameters are reduced by quantum fluctuations. In DP lattices, we find that the exchange interactions favor a quadrupole order.

We further discuss orbital-lattice coupling effects, and show that JT phonon-mediated interactions cooperate with exchange interactions to support quadrupolar order. This is similar to conventional e_g-orbital systems. We suggest that in DP lattices, where the magnetic ions are widely separated and have no common oxygen, a dynamical Jahn-Teller effect may develop to reduce the structural distortions induced by quadrupolar order. We also consider modifications of the pseudospin wave functions by symmetry lowering distortions (caused by site disorder or other defects), and find that they induce a magnetic dipole moment on the E_g doublet. In general, d^2 compounds represent an interesting class of materials where all three main actors—the electron exchange, orbital-lattice interaction, and relativistic SOC—play an essential role in determining the ground states and low-energy excitations.

The paper is organized as follows: Section II introduces the E_g-doublet states and their pseudospin-1/2 description. In Sec. III, we derive pseudospin Hamiltonians considering different orbital exchange geometries, which are typical in TM compounds. Section IV studies pseudospin orderings and excitations on various lattice structures. Section V discusses Jahn-Teller coupling and disorder effects in the context of experiments in DP compounds. Section VI summarizes the main results.

II. NON-KRAMERS E_g DOUBLET AND PSEUDOSPINS

The E_g-doublet wave functions written in the J_z basis are: $\frac{1}{\sqrt{2}}(|2\rangle + |-2\rangle)$ and $|0\rangle$ [6]. These functions follow from diagonalization of the octahedral crystal field operator for $J = 2$ ions [12,22], and as expected on symmetry grounds, are similar to the e_g doublet states of a d electron with $l = 2$. We regard them as pseudospin $s = 1/2$ states $|\uparrow\rangle$ and $|\downarrow\rangle$,

correspondingly. To get an idea about the orbital shapes of the E_g wave functions, we use Clebsch-Gordan coefficients and represent them in terms of two-electron spin and orbital $|S_z, L_z\rangle$ states:

$$|\uparrow\rangle = \frac{1}{\sqrt{2}}(|1, 1\rangle + |-1, -1\rangle), \tag{1}$$

$$|\downarrow\rangle = \frac{1}{\sqrt{6}}(|1, -1\rangle + 2|0, 0\rangle + |-1, 1\rangle). \tag{2}$$

In the pseudospin-up state with $L_z = \pm 1$, one of the electrons must occupy $l_z = 0$ planar orbital $d_0 = d_{xy}$, flattening the overall charge density as shown in Fig. 1(a). However, the pseudospin-down state (2) is dominated by an $L_z = 0$ component $|d_{+1}d_{-1}\rangle$, where the electrons occupy $l_z = \pm 1$ complex orbitals $d_{\pm 1} = \mp(d_{yz} \pm id_{zx})/\sqrt{2}$; thus, its charge density is elongated towards apical oxygen O_z. Under cubic rotations, the E_g wave functions (1) and (2) transform similar to e_g-orbital pair $x^2 - y^2$ and $3z^2 - r^2$.

Within the E_g doublet, the $J = 2$ quadrupole operators

$$O_3 = \frac{1}{6}(2J_z^2 - J_x^2 - J_y^2), \tag{3}$$

$$O_2 = \frac{1}{2\sqrt{3}}(J_x^2 - J_y^2), \tag{4}$$

have matrix elements $\langle \pm \frac{1}{2}|O_3| \pm \frac{1}{2}\rangle = \pm 1$ and $\langle \pm \frac{1}{2}|O_2| \mp \frac{1}{2}\rangle = 1$. Thus, the following correspondence between the pseudospin s^z and s^x components, and E_g quadrupoles follows: $s^z = \frac{1}{2}O_3$ and $s^x = \frac{1}{2}O_2$. The third component $s^y = \frac{1}{2}T_{xyz}$ describes the octupolar moment $T_{xyz} = \frac{1}{\sqrt{3}}\overline{J_xJ_yJ_z}$ with threefold symmetry axis [111]. The projections of the octahedral x, y, z axes onto the two-dimensional pseudospin (s^z, s^x) plane [111] make 120° angles between them, and the pseudospin s^z axis is parallel to the octahedral z axis projection, see Fig. 1(a). This is the most natural choice, because s^z is related to the O_3 quadrupole moment (3) directed along z axis. As we will see below, this also results in one-to-one correspondence between the exchange bond labels $\gamma \in \{x, y, z\}$ and octahedral (x, y, z) axes. The basis rotations within the (s^z, s^x) plane by $\phi = 2\pi/3$ correspond to the cyclic permutations among J_x, J_y, J_z. Finally, we note that the s^z and s^x operators are TR-even, while the s^y octupole is TR-odd; this implies that the pairwise interactions of the type $s_i^z s_j^y$ and $s_i^x s_j^y$ are not allowed, unless TR symmetry is broken.

Following e_g-orbital pseudospin formalism [2,25], we introduce the following pseudospin combinations:

$$\tau_\gamma = \cos\phi_\gamma \, s^z + \sin\phi_\gamma \, s^x, \tag{5}$$

$$\bar{\tau}_\gamma = -\sin\phi_\gamma \, s^z + \cos\phi_\gamma \, s^x. \tag{6}$$

Here, the pseudospin index $\gamma = (z, x, y)$ also specifies the corresponding angles $\phi_\gamma = (0, 2\pi/3, 4\pi/3)$. In essence, $(\tau_\gamma, \bar{\tau}_\gamma)$ play the role of (s_γ^z, s_γ^x) operators defined in the rotated basis

of pseudospin functions:

$$|\uparrow\rangle_\gamma = \cos(\phi_\gamma/2)|\uparrow\rangle + \sin(\phi_\gamma/2)|\downarrow\rangle, \qquad (7)$$

$$|\downarrow\rangle_\gamma = -\sin(\phi_\gamma/2)|\uparrow\rangle + \cos(\phi_\gamma/2)|\downarrow\rangle. \qquad (8)$$

Physically, τ_x (τ_y) and $\bar{\tau}_x$ ($\bar{\tau}_y$) correspond to the quadrupolar operators of $3x^2 - r^2$ ($3y^2 - r^2$) and $y^2 - z^2$ ($z^2 - x^2$) symmetries, respectively. The notations τ_γ and $\bar{\tau}_\gamma$ are useful since one may derive the exchange Hamiltonian $\mathcal{H}^{(\gamma)}$ for $\gamma = z$ type bonds in terms of (s^z, s^x) pair, and then restore $\mathcal{H}^{(\gamma)}$ for all γ by simply replacing $s^z \to \tau_\gamma$ and $s^x \to \bar{\tau}_\gamma$. In perovskites with $180°$ bonding, the z-type bond is parallel to the octahedral z axis; while in other cases, e.g., in a honeycomb lattice, the z-type bond is orthogonal to the octahedral z axis (a convention also used in the Kitaev model literature).

To derive pseudospin exchange interactions, one has to project Kugel-Khomskii type spin-orbital Hamiltonians—which are already known from previous works—onto the low-energy E_g-doublet subspace. We note that conventional e_g-orbital exchange interactions operate in the quadrupolar sector (s^z, s^x) exclusively [2]. In contrast, we will see below that the E_g "orbital" exchange may involve interactions between the octupole moments s^y, as well; this is because the E_g-pseudospin states are spin-orbit entangled objects. Combined with the specific hopping geometry of t_{2g} orbitals, this results in a nontrivial structure of the E_g interactions. We consider below some basic exchange processes, which commonly appear in transition metal compounds.

III. PSEUDOSPIN EXCHANGE HAMILTONIANS

A. Single-orbital exchange: Direct t_{2g} orbital overlap

We start with the simple case where one specific orbital is active on a given nearest-neighbor (NN) exchange bond. Two examples of single-orbital coupling are shown in Fig. 1(b): direct d_{xy}-orbital hopping on z-type bonds in the honeycomb lattice, and d_{xy}-orbital hopping in the ab plane of the DP lattice [24]. In this case, we expect that the E_g exchange Hamiltonian is similar to that for e_g orbitals in ferromagnetic manganites. Indeed, spin-orbit E_g and pure orbital e_g states have the same (Γ_3) symmetry properties. Moreover, the Kugel-Khomskii e_g-exchange process also involves a single-orbital, specific to a given bond [2].

Neglecting Hund's coupling effects in the intermediate states, direct hopping $-t_d(d_{xy,i}^\dagger d_{xy,j} + \text{H.c.})$ gives the following exchange Hamiltonian, written in terms of spin $S = 1$ and orbital $L = 1$ moments of a d^2 ion [26]:

$$\mathcal{H}_{ij}^{(c)} = \frac{t_d^2}{U}\left[(\boldsymbol{S}_i \cdot \boldsymbol{S}_j + 1)L_{zi}^2 L_{zj}^2 - L_{zi}^2 - L_{zj}^2\right]. \qquad (9)$$

For the x (y) bonds where the d_{yz} (d_{zx}) orbital exchange is active, L_z is replaced by L_x (L_y). Projection of this Hamiltonian onto the E_g subspace results in

$$\mathcal{H}_{ij}^{(\gamma)}(d) = J_\tau \, \tau_{i\gamma} \tau_{j\gamma}, \qquad (10)$$

with $J_\tau = \frac{4}{9}\frac{t_d^2}{U}$, and τ_γ given by Eq. (5). This interaction has the same structure as the Kugel-Khomskii e_g-orbital Hamiltonian, but with the reduced exchange constant due to a small fraction of the active orbital (e.g., d_{xy} for the z bond) in

the two-electron E_g wave function. Representative values of $t_d \sim 0.1 - 0.2$ eV and $U \sim 2$ eV would give an energy scale of $J_\tau \sim 2 - 9$ meV (the lower end is appropriate for DP lattice where d-ions are well separated and thus hopping t_d is small).

We note that there is a subtle difference between Eq. (10) and the Kugel-Khomskii e_g exchange in perovskites [2]. In the latter, the active e_g orbital (say $3z^2 - r^2$ on z bond) is quasi-one dimensional and bond-oriented, thus enforcing pseudospins τ_γ to be aligned along the interacting γ-bond directions (hence the name "pseudodipolar" or "compass" model [2]). In contrast, the τ_γ quadrupoles in Eq. (10) try to avoid the bond directions; e.g., for z-type bond we have $s_i^z s_j^z$ coupling but with the Ising s^z axis being perpendicular to the z-bond direction. Physically, the pseudospin orientation specifies the shape of the quadrupolar charge distribution and can be probed in the experiment. Formally however, the two models can be converted into each other by a $90°$ rotation within the (s^x, s^z) quadrupolar plane [i.e., replacing τ in Eq. (10) by $\bar{\tau}$]. This point has to be kept in mind while comparing the present τ model results with those in canonical compass model studies [27–31].

The bond-dependent nature of the interactions in Eq. (10) brings about frustration effects intrinsic to Kugel-Khomskii type spin-orbital models [2] and their descendants [3,31]. Typically, this frustration is resolved by order-from-disorder mechanism, see, e.g., Refs. [32–34].

B. Two-orbital superexchange: 180° bonding geometry

This case is typical for a metal-oxygen-metal (Me-O-Me) superexchange process in perovskites, see Fig. 1(c). On the z-type bond, two orbitals $a = d_{yz}$ and $b = d_{zx}$ equally contribute, and hopping is orbital-conserving: $-t(a_{i\sigma}^\dagger a_{j\sigma} + b_{i\sigma}^\dagger b_{j\sigma})$. The spin-orbital Hamiltonian (at $J_H = 0$) reads as [35]

$$\mathcal{H}_{ij}^{(\gamma)} = \frac{t^2}{U}\left[(\boldsymbol{S}_i \cdot \boldsymbol{S}_j + 1)\mathcal{O}_{ij}^{(\gamma)} + (L_i^\gamma)^2 + (L_j^\gamma)^2\right], \qquad (11)$$

where orbital operator for z type bond reads as

$$\mathcal{O}_{ij}^{(z)} = (L_i^x L_j^x)^2 + (L_i^y L_j^y)^2 + L_i^x L_i^y L_j^y L_j^x + L_i^y L_i^x L_j^x L_j^y. \qquad (12)$$

Operators $\mathcal{O}^{(x)}$ and $\mathcal{O}^{(y)}$ for x and y bonds follow from cubic permutations among L_x, L_y, L_z.

A projection of the above Hamiltonian onto the E_g subspace gives

$$\mathcal{H}_{ij}^{(\gamma)}(180°) = J\left[\boldsymbol{s}_i \cdot \boldsymbol{s}_j + \tfrac{2}{3}\tau_{i\gamma}\tau_{j\gamma}\right], \qquad (13)$$

with the exchange constant $J = \frac{2}{3}\frac{t^2}{U}$. In this equation, the Heisenberg term gives an equal coupling in quadrupolar (s^x, s^z) and octupolar s^y sectors. This term is not present in the Kugel-Khomskii e_g-orbital Hamiltonian, but is realized here because the E_g orbitals have a complex internal structure, and they are made of t_{2g} orbitals with hopping rules different from those for e_g orbitals.

The second bond-dependent τ_γ term in Eq. (13) is a direct analog of the Kugel-Khomskii e_g-orbital exchange. It operates only in the quadrupolar channel, thus disfavoring octupolar correlations. It is important to note that the easy axis orientations in this term exactly coincide with the bond directions,

as dictated by the shapes of the active complex orbitals, e.g., $\mp(d_{yz} \pm i d_{zx})/\sqrt{2}$ orbitals having rotational symmetry around z bond (like $3z^2 - r^2$ axial symmetry in e_g models). Thus the E_g pseudospins in the $180°$ bonding geometry behave exactly as the e_g-orbital compasses do in cubic lattices [2], orienting themselves along the bond directions. This follows from a general observation that in case of axial symmetry, the spin-1/2 anisotropy term should have a dipole-dipole interaction form [36]. For the same reason, the compass-like τ interaction also appears for non-Kramers doublets in f^2 electron system [37]. Due to differences between d- and f-orbital hopping geometries, however, the isotropic term in Eq. (13) is not present in the f^2 case. On square or cubic lattices, we expect that the Hamiltonian (13) would have two-sublattice quadrupolar order, with alternating planar and elongated E_g states, as selected by the anisotropic τ term via order-from-disorder mechanism.

C. Two-orbital superexchange: 90° bonding geometry

This process is typical for nearest-neighbor Me-O$_2$-Me superexchange in delafossite derived structures with edge shared octahedra, see Fig. 1(d). On the z-type bond, two orbitals $a = d_{yz}$ and $b = d_{zx}$ equally contribute again, but hopping is orbital nonconserving: $-t(a_{i\sigma}^\dagger b_{j\sigma} + b_{i\sigma}^\dagger a_{j\sigma})$. The resulting spin-orbital Hamiltonian reads as in the $180°$ case, see Eq. (11), but now with the modified orbital part [i.e., interchanging $L_j^x \leftrightarrow L_j^y$ in Eq. (12)] [35]:

$$\mathcal{O}_{ij}^{(z)} = \left(L_i^x L_j^y\right)^2 + \left(L_i^y L_j^x\right)^2 + L_i^x L_i^y L_j^x L_j^y + L_i^y L_i^x L_j^y L_j^x. \quad (14)$$

The orbital nonconservation during the hoppings has dramatic consequences for the exchange symmetry, as observed previously in spin-orbit $J = 1/2$ [3,38] and $J = 0$ [35] systems. In the present non-Kramers E_g doublet case, this results in the pseudospin Hamiltonian

$$\mathcal{H}_{ij}(90°) = J \left(s_i^y s_j^y - s_i^x s_j^x - s_i^z s_j^z\right), \quad (15)$$

which is completely different from $\mathcal{H}_{ij}(180°)$ in Eq. (13), but the coupling constant remains the same: $J = \frac{2}{3}\frac{t^2}{U}$. This result is remarkable in several aspects. It has no γ-bond dependence, since the quadrupolar (s^x, s^z) part is isotropic and does not change under the rotations (5) and (6), and the octupolar s^y moment is not affected by C_3 rotations around [111] axis and is thus independent of γ as well. This is unlike the d^5 Kramers doublet case, where the cubic rotations affect all three components of the $J = 1/2$ vector, via cyclic permutations of its x, y, z components (see, e.g., Eq. (5.8) in Ref. [3]). Nevertheless, SOC results in strong exchange anisotropy: quadrupoles are ferro-correlated, while the octupolar components s^y are coupled in an antiferro-fashion.

In bipartite (e.g., honeycomb) lattices, this anisotropic Hamiltonian can conveniently be converted into an AF Heisenberg form $J\mathbf{s}_i \cdot \mathbf{s}_j$, by changing the sign of the s^x and s^z components on one of the sublattices; such hidden symmetries are common to spin-orbit pseudospin-1/2 Hamiltonians [3,39,40]. After this transformation, one observes an exact degeneracy between quadrupole and octupolar orderings, with the out-of-plane Goldstone mode representing a smooth rotation from one type order to the other one at no energy cost. Such exact degeneracy and coherent mixture of different

(even/odd) rank order parameters and related gapless modes is rather unusual, but have previously been discussed in the context of t_{2g}-orbital Hamiltonians, see Refs. [3,41] for details.

IV. PSEUDOSPIN ORDER: QUADRUPOLAR VERSUS OCTUPOLAR STATES

In this section, we discuss the phase behavior and excitations of the E_g pseudospin models on different lattices.

A. Simple cubic lattice

The two-orbital $180°$-exchange Hamiltonian (13) is applicable to perovskite lattices. As we already mentioned in that section, we expect a two-sublattice quadrupolar order in this case. This is conceptually similar to e_g-orbital order in $3d$ systems; the only difference is that the E_g "orbitals" are spin-orbit coupled objects. Like in the e_g-orbital case, both exchange and JT couplings will contribute to the quadrupolar ordering, and they typically support each other. Formally, the Hamiltonian (13), comprising an AF Heisenberg interaction and an anisotropic compass-like terms is very similar to the model studied in Ref. [32]. Thus, its excitation spectrum should acquire a sizable gap due to the order-by-disorder mechanism.

B. Honeycomb lattice

A honeycomb lattice is derived from the delafossite structure with edge-shared octahedra. In general, two different channels are operative in this case: direct hopping t_d considered in Sec. III A, and indirect t superexchange via $90°$ bonding considered in Sec. III C. It is known that for pseudospin $J = 1/2$ exchange in d^5 compounds, there is also a combination of these two processes (i.e., t times t_d terms) resulting in the off-diagonal, so-called Γ interaction [42]. Interestingly, such a crossterm is absent in the present E_g problem. So, the full Hamiltonian in honeycomb or triangular lattices is comprised of the bond-dependent τ model (10), and the $90°$ exchange J interaction (15), which is also anisotropic, but bond-independent:

$$\mathcal{H}_{ij}^{(\gamma)} = J_\tau\, \tau_{i\gamma}\tau_{j\gamma} + J\left(s_i^y s_j^y - s_i^x s_j^x - s_i^z s_j^z\right). \quad (16)$$

Physically, both J_τ and J are positive, and their ratio can be arbitrary. While the first term operates in the pure quadrupolar (s^z, s^x) sector, J coupling equally supports AF octupolar and FM quadrupolar states. As noticed above, the J interaction is actually dual to the AF Heisenberg model (on bipartite lattices). A finite τ term breaks this symmetry and selects the ordering type. Since the (s^z, s^x) part of the J term has a negative sign, a small admixture of positive J_τ reduces the quadrupole interactions. As a result, two-sublattice staggered order of octupole moments s^y is favored at $J \gg J_\tau$. The ground state wave function is complex, $\psi_{A/B} = (|\uparrow\rangle \pm i|\downarrow\rangle)/\sqrt{2}$, and has a cubic shape, see Fig. 2(c) of Ref. [4].

In the opposite limit $J_\tau \gg J$, it is obvious that s^y octupole order has to give way to ordering of the τ quadrupoles that live in (s^z, s^x) plane. The quadrupole order is TR invariant

(i.e., the condensate wave function is real) but breaks cubic symmetry. The transition is of a spin-flop type: spins flop from the [111] direction into the honeycomb plane. In terms of the condensate wave function, this corresponds to the phase-jump from $\pi/2$ to 0 in the relative phase factor $e^{i\phi}$ between $|\uparrow\rangle$ and $|\downarrow\rangle$ states.

Interestingly, the transition point and quadrupole order pattern that replaces octupole order can be obtained from symmetry considerations alone, by virtue of the duality transformations in pseudospin honeycomb models [40]. To this end, we use the explicit form of τ_γ given in Eq. (5) and rewrite Eq. (16) as follows:

$$\mathcal{H}_{ij}^{(\gamma)} = (1-\lambda)\left(s_i^z s_j^z + s_i^x s_j^x\right) + \lambda s_i^y s_j^y$$
$$+ \cos\phi_\gamma\left(s_i^z s_j^z - s_i^x s_j^x\right) - \sin\phi_\gamma\left(s_i^z s_j^x + s_i^x s_j^z\right). \quad (17)$$

Here, $\lambda = 2J/J_\tau$, and the overall energy scale equal to $J_\tau/2$ is not shown. This equation has exactly the same structure as the extended Kitaev model, written in the hexagonal coordinate frame [40]. Simple relabeling of the spin axes $(x, y, z) \leftrightarrow (Y, Z, X)$, and a term-by-term comparison of Eq. (17) with Eq. (A1) of Ref. [40] gives the following correspondence: $J_{XY} = 1 - \lambda$, $J_Z = \lambda$, $A = 1$, and $B = 0$. (We note that B term of Ref. [40] couples in-plane and out-of-plane components of spins; for the present E_g problem, finite B would imply linear quadrupole-octupole coupling, which is forbidden by TR symmetry). Next, we use the relations (A2–A5) of Ref. [40] to obtain the parameters K, Γ, $\bar{J}$, and Γ', which define the extended Kitaev model in the octahedral axes frame [42] (we use $\bar{J}$ to avoid confusion with J in our models):

$$K = 1, \quad (18)$$

$$\Gamma = 1 - \tfrac{2}{3}(1-\lambda), \quad (19)$$

$$\bar{J} = \tfrac{1}{3}(1-\lambda), \quad (20)$$

$$\Gamma' = -\tfrac{2}{3}(1-\lambda). \quad (21)$$

So far, we have shown that Eqs. (16) and (17) correspond to the extended Kitaev model at the specific parameter set. The virtue of this mapping is that at $\lambda = 2J/J_\tau = 1$, we see that $\bar{J} = \Gamma' = 0$. Thus, at this point, the model is isomorphic to the $K = \Gamma = 1$ model, which in turn, is dual to the isotropic Heisenberg model, see Table I of Ref. [40]. This leads to a remarkable observation that at $J_\tau = 2J$, the highly anisotropic Hamiltonian (16) is dual to the effective FM Heisenberg model $\tilde{\mathcal{H}}_{ij} = -J\tilde{s}_i \cdot \tilde{s}_j$. The duality transformation involves a six-sublattice rotation matrix $\mathcal{T}_6$ [40], which converts in-plane FM order of effective spins $\tilde{s}$ into a vortex pattern of s^z and s^x moments in our model. This quadrupole order is shown in Fig. 2(a) (cf. Fig. 2(e) of Ref. [40]). On the other hand, out-of-plane FM order of $\tilde{s}$ corresponds to octupolar AF order of s^y moments already discussed above. Being dual to the eigenstates of a hidden FM Heisenberg model, these vortex and AF states are "fluctuation free", and low-energy excitations are magnons with a quadratic dispersion.

The exact degeneracy of these two states is lifted as soon as λ deviates from its critical value 1. From Eq. (17), we see that the corrections to the SU(2) point Hamiltonian $\mathcal{H}(\lambda = 1)$ read as $(1-\lambda)(s_i^z s_j^z + s_i^x s_j^x - s_i^y s_j^y)$. This term acts as an easy-plane
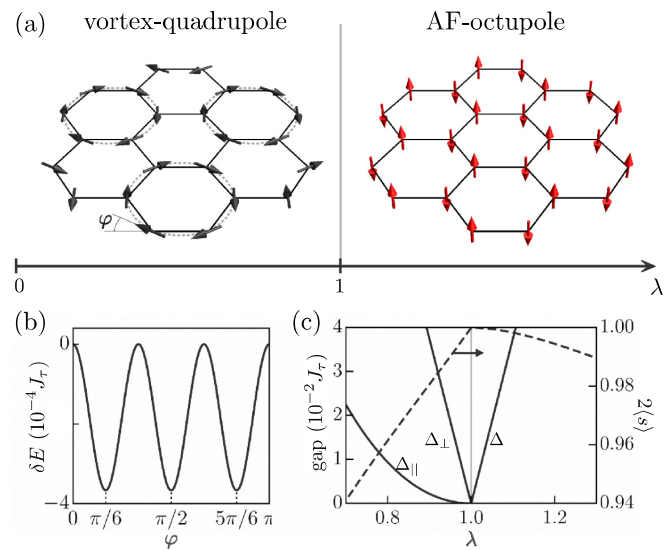

FIG. 2. (a) Phase diagram of the Hamiltonian (17) on honeycomb lattice as a function of $\lambda = 2J/J_\tau$. There are two states, separated by a first-order spin-flop transition at the hidden SU(2) symmetric point $\lambda = 1$. Left and right insets show the ordered patterns of the vortex-type quadrupole and AF-octupole phases, respectively. (b) Quantum zero-point energy δE as a function of ordered moment orientation φ within the honeycomb plane, calculated at $\lambda = 0.5$. A ground-state pattern with $\varphi = \pi/6$ is shown in panel (a) left. (c) The in-plane ($\Delta_\parallel$) and out-of-plane ($\Delta_\perp$) magnon gaps in the vortex-quadrupole phase, and the magnon gap (Δ) in the uniaxial AF-octupole ordered state. Dashed line shows the pseudospin order parameter length $2\langle s \rangle$ near the transition point, where the model is dual to a fluctuation free Heisenberg FM.

or easy-axis anisotropy, selecting quadrupolar vortex order if $1 - \lambda > 0$, and s^y octupolar AF order if $1 - \lambda < 0$. It also opens a finite gap in magnon spectra.

The symmetry-based considerations above are confirmed by numerical studies. Figure 2(a) shows the phase diagram of Hamiltonian (17), obtained by classical theory and exact diagonalization on a C_3 symmetric 24-site cluster. The first-order transition between the vortex-quadrupole and AF-octupole phases occurs at $\lambda = 1$. Across the spin-flop transition, the in-plane quadrupole moments (black arrows) flip to the out-of-plane octupole moments (red arrows). We investigated the quantum effects using linear spin wave theory (LSWT). In the quadrupole phase, the zero-point magnon energy δE depends on the vortex pattern orientation [specified by the angle φ in Fig. 2(a)]. The state with $\varphi = \pi/6$ has the lowest energy, see Fig. 2(b). Note that the pinning potential is extremely weak, so the spins are almost free to rotate (globally) within a quadrupolar plane. This implies the presence of low-energy quadrupole moment fluctuations.

The calculated magnon gaps are presented in Fig. 2(c) near the spin-flop transition area ($\lambda \sim 1$). In the planar-type quadrupole phase, there are two different gaps, $\Delta_\perp$ and $\Delta_\parallel$, associated with the out-of-plane and in-plane magnon modes. The out-of-plane gap is finite already within LSWT, and proportional to the deviation from the hidden FM SU(2) point: $\Delta_\perp \propto (1-\lambda)$. The in-plane gap, on the other hand, is zero within LSWT because the classical energy of the vortex
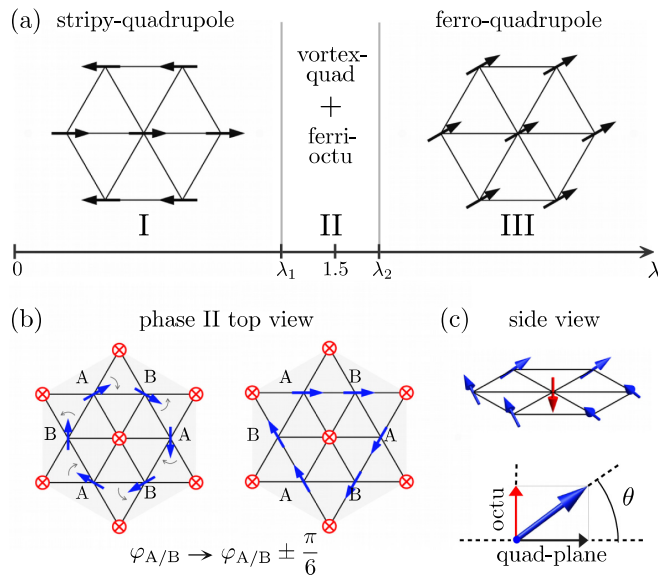
FIG. 3. (a) Phase diagram of Hamiltonian (17) on the triangular lattice as a function of $\lambda = 2J/J_\tau$. The phases are separated by spin-flop transitions at λ_1 and λ_2. Insets: The ordering patterns of phases I and III. (b) Magnetic unit cell in the quadrupole-octupole mixed phase II. Triangular sublattice (red circles) is occupied by down-oriented octupole moments. On a hexagon, the in-plane components of spins form a vortex. Left and right patterns are related by in-plane φ rotations, in opposite directions on A and B sites; quantum effects slightly favor the right pattern. (c) Upper part: Down-oriented octupole moment at the center, and out-of-plane canted spins (blue arrows) on a hexagon. Lower part: Decomposition of a canted spin into octupole and quadrupole moments.

pattern is independent of the in-plane rotation angle φ. Planar anisotropy $\delta E(\varphi)$ and the corresponding gap only appears beyond LSWT level, via quantum order-from-disorder mechanism, and thus is small: $\Delta_\parallel \propto (1-\lambda)^2$. The octupole phase ($\lambda > 1$) has uniaxial symmetry and a two-fold degenerate magnon dispersion with the gap $\Delta \propto (\lambda - 1)$. As expected, the ordered moments (dashed line) are fully saturated at the hidden FM point. Away from this point, they are reduced by quantum fluctuations (the effect is stronger in the quadrupole phase owing to the presence of a soft in-plane magnon mode).

C. Triangular lattice

The behavior of the model (16), or its equivalent (17), on a triangular lattice is of interest too. It is also relevant to double-perovskites, where the face-centered-cubic (fcc) lattice of magnetic ions can be viewed as triangular planes stacked along the [111] direction. The triangular lattice is nonbipartite and a paradigmatic example of geometrical frustration for AF Ising-type models. This is exactly the case for octupolar interactions here: see the $Js_i^y s_j^y$ or $\lambda s_i^y s_j^y$ terms with positive J and λ values in Eqs. (16) and (17), respectively.

Leaving full exploration of the model for future study, we discuss now its global phase behavior on a triangular lattice. Inspection of the classical ground states, supported by classical Monte Carlo simulations suggest that there are (at least) three distinct phases, shown in Fig. 3(a), which

are realized when the parameter $\lambda = 2J/J_\tau$ varies from pure J_τ limit to a dominant J regime. Stripy-quadrupole phase I at small λ is essentially the same state as found earlier in compass model [29,30]; note, however, that the spin pattern in our "anticompass" τ model is rotated by 90°, for the reasons discussed in Sec. III A. This state has a classical energy per site $E_I = -(3-\lambda)s^2$ (in units of $J_\tau/2$).

At large λ, the ground state is driven by the J interaction, which is of ferro-type in the quadrupolar channel, while octupole AF coupling is equally strong but frustrated. This results in simple ferro-quadrupole order (phase III), with energy $E_{III} = -3(\lambda - 1)s^2$. Classically, moments can freely rotate within a quadrupolar plane, but quantum effects generate in-plane anisotropy, pinning the ordered moments along the middle of the two bonds ($\varphi = \frac{\pi}{6}$). The anisotropy is rather weak: magnon zero-point energy, calculated at $\lambda = 2$, varies only by $\delta E(\varphi) \simeq 7 \times 10^{-4} J_\tau$.

In the above states I and III, the octupolar Ising interaction $\lambda s_i^y s_j^y$ was left "unused" because of its frustrating nature. At intermediate λ values, however, this coupling is actually larger than the quadrupolar one (as J_τ and J quadrupole terms are of different sign and compete). Therefore, an intermediate state between I and III, which finds a way to resolve "triangular" frustration and activates large octupole couplings, is expected.

The pseudospin ordering pattern, whose unit cell is shown in Fig. 3(b) and further detailed in Fig. 3(c), does exactly this job. In this state, the original triangular lattice is divided into two, honeycomb and triangular sublattices. The spins on the honeycomb sublattice are canted and carry both octupole and quadrupole moments. The latter condense into a vortex pattern similar to what shown in Fig. 2(a). While the out-of-plane components form a ferro-octupole order. The honeycomb octupole moment is largely (but not fully) compensated by down-oriented octupoles residing at the middle of every hexagon. As a whole, phase II represents a coherent superposition of vortex-quadrupole and ferri-octupole orders. Such a mixture of the different rank multipoles is rather unusual. We also note that this order is noncoplanar and has a large unit cell, which helps to relieve the frustrations inherent to spin-orbital models. In this sense, the case is similar to a complex behavior of spin-orbit pseudospins $J = 1/2$ of d^5 ions on a triangular lattice [3,43,44].

As a function of spin canting angle θ, the classical energy of the mixed state II is obtained as follows:

$$E_{II}(\theta)/s^2 = -1 - 2\lambda \sin\theta + (1 + \lambda)\sin^2\theta. \quad (22)$$

Here, the second term originates from coupling between honeycomb lattice octupoles $s^y \propto \sin\theta$ with those residing at the hexagon centers. Minimizing $E_{II}(\theta)$ with respect to θ, we find $\sin\theta = \lambda/(1 + \lambda)$. This gives a ground state energy of phase II (per site):

$$E_{II} = -\left(\lambda + \frac{1}{1+\lambda}\right)s^2. \quad (23)$$

Comparing this result with E_I and E_{III} obtained above, we find the phase transition points λ_1 and λ_2:

$$\lambda_1 = \frac{1 + \sqrt{17}}{4} \simeq 1.28, \quad \lambda_2 = \frac{1 + \sqrt{33}}{4} \simeq 1.69. \quad (24)$$

In between λ_1 and λ_2, the angle θ varies from $34°$ to $39°$, and the size of octupole moment on honeycomb sites $2|\langle s^y \rangle| = \sin \theta \simeq 0.56 - 0.63$. This nearly compensates pure octupole moments from triangular sublattice, leaving rather small total octupole moment per site: $2|\langle s^y \rangle|_{tot} = \frac{1}{3}(2 \sin \theta - 1) \simeq 0.04 - 0.09$.

Displayed in Fig. 3(b) are two different vortex patterns, related to each other by in-plane rotations of spins. Classically, these states are degenerate. Quantum zero-point energies, calculated within LSWT for these two ground states, slightly differ; the right one is lower by $\delta E \simeq 2 \times 10^{-4} J_\tau$. This result implies that in-plane magnon excitations acquire a small but finite gap, generated by the order-from-disorder mechanism. Out-of-plane excitations, corresponding to fluctuations between quadrupole and octupole sectors, are gapped out already on a classical level.

Overall, the E_g pseudospin $J_\tau - J$ model (16) on triangular lattice contains rich physics yet to be fully explored theoretically. The above results also should encourage experimental work finding and studying $5d^2$ compounds with quasi-two dimensional honeycomb and triangular lattice structures.

D. Double perovskites

Now, we move to the DP lattice, which motivated this study. DPs are special because the magnetic ions are widely separated from each other and thus interact weakly. This implies that the pseudospin one-half description, which assumes that the intersite interactions are less than on-site cubic splitting Δ_c, is best justified in DP compounds.

The dominant exchange channel in DPs is due to the single-orbital process considered in Sec. III A. This results in Kugel-Khomskii type Hamiltonian (10) acting in the pure quadrupole τ-channel: $J_\tau \tau_{i\gamma} \tau_{j\gamma}$. To our knowledge, the ground state of this model on fcc lattice (formed by magnetic ions in DPs) has not yet been considered. To address the behavior of the τ model on the highly frustrated fcc lattice, we perform classical Monte Carlo simulations on the related model, $J_\tau n_{i\gamma} n_{j\gamma}$, where pseudospins $\tau = 1/2$ are replaced by classical vectors of unit length ($\boldsymbol{n}^2 = 1$).

The simulated annealing Monte Carlo is performed for DP and, for comparison, triangular lattices. We use 1372 sites ($7 \times 7 \times 7$ unit cell) of DP and 1296 sites (36×36) of triangular lattice with periodic boundary conditions. Monte Carlo simulations were performed using the ALPS project library [45–47]. We find a collinear AF-quadrupole order at low temperatures, and the ordering pattern in DP lattice is displayed in Fig. 4(a). The moment is along the bond direction, and there are 8 antiparallel and 4 parallel nearest neighbors. Within the [111] planes, moments form a stripy pattern as in the triangular lattice, see phase I in Fig. 3(a). Temperature dependence of the ordered moment length $\langle n \rangle$ in Fig. 4(b) shows that the ordering sets in at $T_c \simeq 1.6 J_\tau$ in DP lattice. This is about three times higher than T_c / J_τ in the triangular lattice, most likely due to increased dimensionality. Quantifying the quadrupole moment reduction by quantum fluctuations in fcc lattice is an interesting but challenging problem, and left for future study.

It should also be noticed that T_c in the actual model with quantum spin $\tau = 1/2$ is different from the above Monte
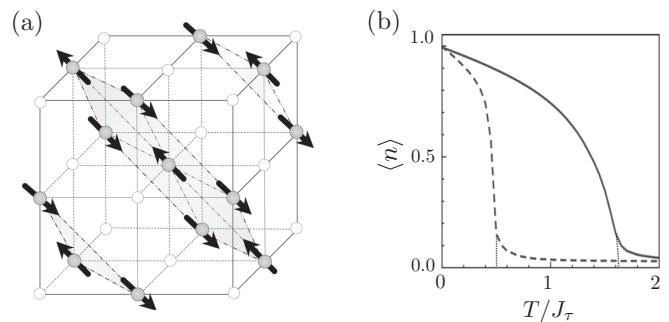

FIG. 4. (a) Double perovskite lattice, where the transition metal ions (filled circles) reside on the fcc sublattice. Arrows show the ordered pattern of quadrupole moments. It can be viewed as a stack of triangular lattice [111] planes (shaded), with stripy-AF quadrupole order within each plane. (b) Temperature dependence of the order parameter $\langle n \rangle$ for classical J_τ model in DP (solid line) and triangular (dashed line) lattices, obtained by classical Monte Carlo simulation.

Carlo result. Roughly, an upper limit for the rescaling factor can be obtained by replacing $\boldsymbol{n}^2 = 1$ by $s(s + 1)$. For the present case of spin one-half, this gives an estimate of $T_c \sim J_\tau$. A rather low value of T_c (despite a large coordination number 12) is presumably due to frustrations of the model on fcc lattice.

In principle, the $90°$ bonding superexchange via nonmagnetic B' sites is possible in DP lattice, due to the extended nature of $5d$ orbitals. However, this process involves many hopping steps (B_i-O-B'-O-B_j), and the corresponding indirect hopping t and hence J are expected to be small. Therefore, even though the full exchange Hamiltonian in DPs is formally given by Eq. (16), the single-orbital quadrupole interaction J_τ should dominate over J coupling between the octupoles. (This can be contrasted to the f^2 ion exchange in the fcc lattice, which is dominated by octupole interaction [37]). Our result implies that spin-orbital exchange in DPs uniquely supports AF order of quadrupole moments, breaking underlying discrete point group symmetries both in real and pseudospin spaces, but preserves TR symmetry.

We should note that the above result is obtained at large cubic splitting Δ_c between the excited T_{2g} states and pseudospin E_g doublet. The previous calculations in the other limit, i.e., neglecting cubic splitting and using full $J = 2$ Hilbert space instead [24] found no octupolar instability, too. Reference [22] suggested that in the intermediate case, when the E_g doublet is formed and T_{2g} triplet is not too high, the virtual states may generate octupolar interactions that are strong enough to overcome quadrupolar couplings. We now inspect this possibility, by considering contributions of the virtual T_{2g} states to the effective pseudospin E_g Hamiltonian. This brings us to Jahn-Teller physics, which operates not only within the ground state E_g doublet, but also connects it with the T_{2g} triplet.

V. JAHN-TELLER COUPLING EFFECTS. IMPLICATIONS FOR DOUBLE-PEROVSKITES

A. Jahn-Teller Hamiltonian

We consider a linear coupling between the octahedral normal modes Q_Γ and electron quadrupolar moments O_Γ of

symmetry Γ. For t_{2g}-orbital systems, the Γ_3 doublet (Q_3 and Q_2 modes of $3z^2 - r^2$ and $x^2 - y^2$ symmetries, respectively) as well as Γ_5 triplet modes (Q_{xy}, etc.) are relevant [6]. Microscopically, orbital-lattice coupling in the Γ_3 channel splits the t_{2g}-orbital levels, while coupling to Γ_5 modes is orbital nondiagonal, e.g., Q_{xy} distortion mixes d_{yz} and d_{zx} wave functions.

In terms of two-electron $J = 2$ quadrupoles, the Jahn-Teller couplings in the above two channels read as follows (summation over lattice sites i is implied):

$$\mathcal{H}_{JT}(\Gamma_3) = -g\,(Q_3 O_3 + Q_2 O_2)_i, \tag{25}$$

$$\mathcal{H}_{JT}(\Gamma_5) = -g'(Q_{xy}O_{xy} + Q_{yz}O_{yz} + Q_{zx}O_{zx})_i, \tag{26}$$

where O_3 and O_2 quadrupoles are defined in Eqs. (3) and (4), while $O_{xy} = (J_x J_y + J_y J_x)/2\sqrt{3}$, etc. Within the ground-state E_g doublet, Γ_3 coupling takes a form familiar from the e_g-orbital JT problem [2,25]:

$$\mathcal{H}_{JT}(\Gamma_3) = -g\,(Q_3 \sigma^z + Q_2 \sigma^x), \quad \sigma^{z/x} = 2s^{z/x}. \tag{27}$$

On the other hand, quadrupolar operators in $\mathcal{H}_{JT}(\Gamma_5)$ have no matrix elements within the pseudospin subspace; instead, they connect the E_g doublet to the excited T_{2g} states. This leads to a so-called second-order or "pseudo-Jahn-Teller" effect [48], which operates through the mixing of the ground and excited states. In spin-orbit coupled systems, this effect modulates the spatial shape of the pseudospin wave functions and generates new terms in low-energy effective Hamiltonians [49].

B. Pseudospin interactions mediated by Jahn-Teller coupling

Spatial correlations between the octahedral deformations on different sites mediate interactions between quadrupolar moments [10,25,50]. Typically, these interactions cooperate with the Kugel-Khomskii mechanism of orbital ordering [2]. In most TM compounds, the JT centers share common oxygens and thus stay in direct contact with each other. This leaves little room for single-ion JT dynamics. In the DP lattice, however, the JT ions have no common oxygen, so they have to interact by exchanging virtual phonons. Since JT phonon modes disperse weakly, this interaction is much smaller than in perovskites. This has two important consequences: (i) cooperative JT couplings are weak enough so that the E_g-pseudospin description remains valid, and (ii) single-ion JT dynamics, intrinsic to non-Kramers E_g states, may develop.

We start with pseudospin interactions mediated by JT coupling in the Γ_3 channel (27). Two ions in the xy plane couple most efficiently via Q_3 type distortions, as illustrated in Fig. 5(a). The corresponding quadrupole interaction is

$$V\sigma_i^z \sigma_j^z = 4V s_i^z s_j^z, \tag{28}$$

whose strength $V = -g^2 \langle Q_{3i} Q_{3j} \rangle_{\omega=0} > 0$ is given by nonlocal static susceptibility of the Q_3 modes. In DPs, antiferro-type intersite correlations $\langle Q_{3i} Q_{3j} \rangle < 0$ arise due to a finite dispersion $\delta\omega_q$ of the corresponding optical phonons with energy ω_0. This gives a rough scale of V as a small fraction $\propto \delta\omega_q/\omega_0 \sim 0.1$ of a single-ion JT stabilization energy E_{JT}. For d^1 Os in DPs, Refs. [51,52] evaluated $E_{JT} \sim 20$ meV (this might be lower for d^2), suggesting $V \sim 1$ meV, i.e., of the same order as the exchange coupling J_τ for DPs. Relatively
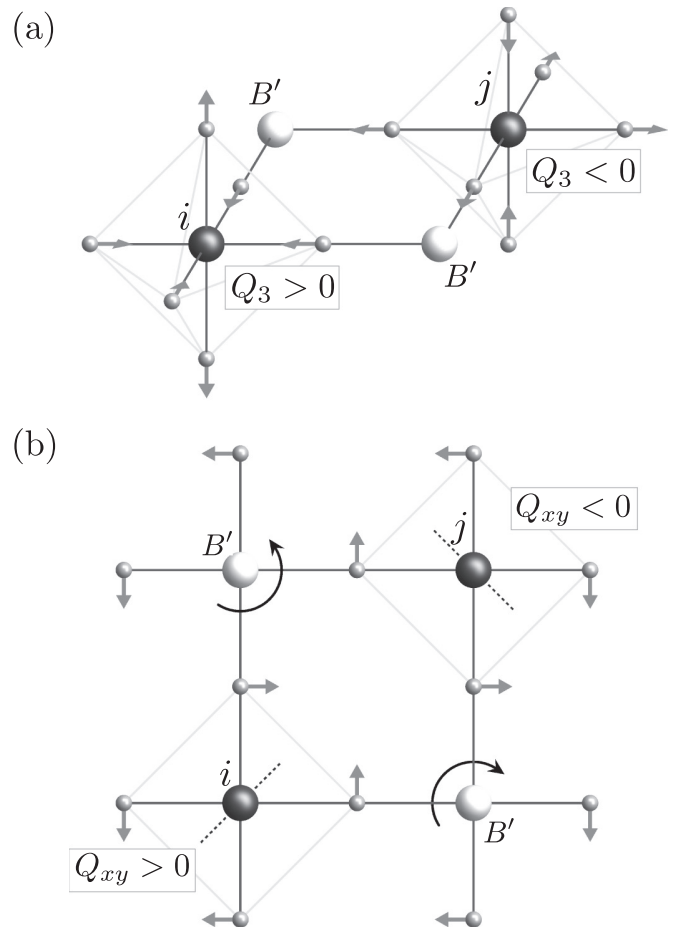

FIG. 5. (a) Antiferro correlated Q_3 distortions on xy plane of the DP lattice, leading to V coupling (28) between quadrupole moments of Γ_3 symmetry. (b) Antiferro correlated Q_{xy} distortions on xy plane, leading to V' coupling (29) in the Γ_5 quadrupolar channel.

small values of E_{JT} (and hence JT mediated coupling V) may indicate a rather weak coupling of the diffuse $5d$ orbitals to the lattice. We note that considering both Q_3 and Q_2 modes would induce also $s_i^x s_j^x$ and $s_i^z s_j^x$ type terms; however, these are not essential in the context of possible octupole order. The main result is that the quadrupole interactions, mediated by Γ_3 type JT phonons cooperate with the exchange coupling, i.e., $J_\tau \rightarrow J_\tau + 4V$, as in the case of the usual e_g-orbital problem in manganites. In general, octupolar order has better chances in systems where Jahn-Teller coupling is inactive or reduced. An example of this is d^1 perovskite Sr_2VO_4 [53], where V^{4+} ion with Kramers doublet ground state is free of JT effect.

The Jahn-Teller coupling in the Γ_5 channel (26) works differently, and it actually leads to octupolar coupling $s_i^y s_j^y$ by virtue of pseudo-JT effect. For a pair in the xy plane, we consider that Q_{xy} type distortions shown in Fig. 5(b) are most relevant. This leads to the following interaction between Γ_5-type quadrupole moments:

$$V' O_{xy}^i O_{xy}^j, \tag{29}$$

with positive $V' = -(g')^2 \langle Q_{xy}^i Q_{xy}^j \rangle_{\omega=0}$. The interactions on yz and zx planes are induced by Q_{yz} and Q_{zx} type modes. For

t_{2g}-orbital systems, constants V and V' are expected to be of the same order, but their ratio depends on material details. In d^1 Os double-perovskite, coupling to Γ_3 type modes are stronger [51], which might also be the case in d^2 osmates.

As said above, Γ_5 quadrupoles have no matrix elements within E_g doublet; instead, they create transitions from the E_g doublet to excited T_{2g} states. For example, $O_{xy} = i(T_z^\dagger f_\downarrow - f_\downarrow^\dagger T_z)$, where hard-core bosons f and T belong to pseudospin ($f_\uparrow, f_\downarrow$) and triplet (T_x, T_y, T_z) sectors, correspondingly. Thus, the pairwise interaction $V' O_{xy}^i O_{xy}^j$ may (a) excite a pair of triplons, and (b) lead to dispersion and broadening of the T excitons. In the present context, we are interested in the pair generation process, which dynamically mixes up the ground- and excited-state wave functions, modifying thereby the pseudospin exchange Hamiltonian. Specifically, this process activates the composite operators $(SL_z^2)_i$ and $(SL_z^2)_j$ in the exchange Hamiltonian of Eq. (9). These operators have non-diagonal $E_g \leftrightarrow T_{2g}$ matrix elements [e.g., $S_z L_z^2 = -(T_z^\dagger f_\uparrow + H.c.)$], and are thus sensitive to the admixture of JT induced triplet states in pseudospin wave functions.

Now, we assume that the exchange J_τ and quadrupole V' couplings are small compared to cubic splitting Δ_c. In other words, we assume that the dispersion and broadening of triplon excitations, caused by these interactions, is smaller than Δ_c, and thus the pseudospin description is valid. This is exactly what is observed in experiment [12]. Then we proceed along the lines of Ref. [22], eliminating virtual triplon pairs perturbatively. This results in the following effective Hamiltonian (for pairs on the xy plane), which now includes the exchange as well as JT-coupling mediated interactions:

$$\mathcal{H}_{\text{eff}}^{(z)} = J_z s_i^z s_j^z + J_x s_i^x s_j^x - J_y s_i^y s_j^y. \tag{30}$$

For $\gamma = x, y$ bonds, one has to replace $s^z \to \tau_\gamma$ and $s^x \to \bar{\tau}_\gamma$. Effective parameters read as

$$J_z = J_\tau \left(1 - \frac{81}{32} \frac{J_\tau}{\Delta_c}\right) + 4V \left(1 - \frac{V'}{8V} \frac{V'}{\Delta_c}\right), \tag{31}$$

$$J_y = J_x = J_\tau \frac{9V'}{4\Delta_c}. \tag{32}$$

Provided that the triplet excitations are well separated from the pseudospin doublet, i.e., J_τ and V' much smaller than Δ_c, the corrections $\propto 1/\Delta_c$ to J_z in Eq. (31) can be neglected, and we obtain

$$\frac{J_y}{J_z} \simeq \frac{J_\tau}{J_\tau + 4V} \frac{2V'}{\Delta_c} < 1. \tag{33}$$

This implies that quadrupolar τ interactions dominate over those in the octupolar s^y sector. Moreover, J_y/J_z ratio can be further reduced by dynamical JT effects, which suppress the interactions involving s^y operators by the Ham factor [6] and discourage the octupole order. The result (33) is natural for $5d$ ions on DP lattices, where intersite interactions J_τ, V, and V' between widely-separated ions should be much less than the single-ion energy Δ_c. The latter is driven by large SOC for $5d$ electrons; we also think that the cubic splitting Δ_c is further enhanced by the dynamical JT effect stabilizing the E_g doublet against the T_{2g} states. It would be interesting to check the latter point by quantum chemistry calculations.

The above findings suggest that a single phase transition observed in $5d^2$ osmium DP oxides [12] is driven by a quadrupolar ordering of E_g doublets. Comparison of the Monte Carlo result (Sec. IV D) for the quadrupolar ordering temperature $\sim J_\tau + 4V$ (including now JT-phonon mediated coupling V) with the experimental transition temperature $30 - 50$ K gives $J_\tau + 4V \sim 4$ meV, consistent with the above estimates of intersite couplings. Concomitant lattice distortions might be small for several reasons: First, JT coupling is already weakened by the SOC effect, which partially removes orbital degeneracy. Second, on-site JT vibronic dynamics [6,48] and intersite quantum fluctuations reduce the pseudospin order parameter and hence the static distortions, to the levels that are difficult to detect directly by x-ray diffraction. In general, JT coupling seems to be rather weak for $5d$ orbitals; indeed, quadrupole order induced distortions in $5d^1$ DPs have been found to be extremely small [18] or below the resolution limit [19]. However, quadrupolar order should lead to changes in phonon spectra that should be well visible in Raman and optical data. Possible signatures of the dynamical JT effect, e.g., transitions between vibronic levels [54] are of special interest. Also, a quadrupolar order can be probed by nuclear magnetic and quadrupole resonance experiments. Further experiments, especially on single crystal samples, are necessary to identify the nature of the "hidden" order parameter in DP $5d^2$ compounds.

C. Coupling to local distortions: Induced magnetic moments

While a quadrupole order of JT active E_g doublets sounds natural, this picture cannot explain TR-symmetry breaking observed in $5d^2$ DPs [13–15]. One possible explanation is to attribute this effect to magnetic moments induced by defects (e.g., $B \leftrightarrow B'$ site disorder). Near defects, noncubic crystal fields can modify the E_g-doublet wave functions, or even completely destroy the pseudospin description, thus recovering the $\boldsymbol{J}$ dipole moments at least partially. Nuclear magnetic and quadrupole resonance lineshapes may quantify such magnetic state inhomogeneities. In fact, the signatures of spin disorder and freezing are rather common in d^2 DPs [13–15]. To show how symmetry lowering distortions affect the physical content of the E_g doublets and their interactions, we consider JT coupling of Γ_5 symmetry quadrupoles $O_{\alpha\beta}$ to the corresponding local distortions $e_{\alpha\beta}$:

$$\delta\mathcal{H}_i = -g'(e_{xy}O_{xy} + e_{yz}O_{yz} + e_{zx}O_{zx})_i. \tag{34}$$

The local quadrupolar fields (34) modify the E_g doublet functions at site i as follows:

$$|\tilde{\uparrow}\rangle_i \Rightarrow |\uparrow\rangle + is(\delta_x|T_x\rangle - \delta_y|T_y\rangle)_i, \tag{35}$$

$$|\tilde{\downarrow}\rangle_i \Rightarrow |\downarrow\rangle + i(\delta_z|T_z\rangle - c\delta_x|T_x\rangle - c\delta_y|T_y\rangle)_i, \tag{36}$$

where $s = \sqrt{3}/2$, $c = 1/2$ [the normalization factors $p_\uparrow^2 = 1 + s^2(\delta_x^2 + \delta_y^2)$ and $p_\downarrow^2 = 1 + \delta_z^2 + c^2(\delta_x^2 + \delta_y^2)$ are not shown]. The parameters $\delta_z = g'e_{xy}/\Delta_c$, etc quantify the degree of admixture of virtual triplet states T_x, T_y, and T_z into the ground state due to strain $e_{\alpha\beta}$ field. This admixture "magnetizes" the E_g doublet, by inducing a dipolar component into the s^y operator. By calculating matrix elements of total angular momentum $\boldsymbol{J}$ within the modified E_g doublet (35, 36),

we find an induced moment $J_{i\alpha} = 4\delta_{i\alpha}s_i^y$, illustrating a partial recovery of the dipolar moments due to local distortions. The corresponding magnetic moment, which is carried by the s^y operator, is $M_{i\alpha} = 2\delta_{i\alpha}s_i^y$ (using g factor $g = 1/2$ of $J = 2$ state).

In principle, a direct link between lattice distortions and magnetism is generic to all spin-orbit Mott insulators. In $5d^2$ ion systems, where the nonmagnetic nature of the E_g doublet is protected by cubic symmetry (i.e., independent of covalency, etc.), lattice distortions have an especially strong impact on magnetic properties. To illustrate this point further, we may consider uniform strain applied along the [111] axis of a crystal: $e_{xy} = e_{yz} = e_{zx} = e/\sqrt{3}$. This induces a magnetic moment with g factor $g_\parallel = \frac{2}{\sqrt{3}}\frac{\Delta_{tr}}{\Delta_c}$, where $\Delta_{tr} = g'e$ is the strain induced field, while the g factors within the [111] plane remain zero. This results in an extreme anisotropy of the magnetic response to lattice distortions in $5d^2$ systems.

Noncubic crystal fields also induce new couplings between pseudospin moments. Projection of the exchange interaction (9) onto the E_g doublet with "distorted" wave functions (35, 36) modifies the J_τ term in Eqs. (10) and (16) as follows:

$$J_\tau \; \tau_{i\gamma}\tau_{j\gamma} \rightarrow J_\tau\big[\tau_{i\gamma}\tau_{j\gamma} + a_{ij}^{(\gamma)}s_i^y s_j^y\big], \qquad (37)$$

where a new term, the $s_i^y s_j^y$ coupling, which operates in the magnetic channel, appears. Its relative strength is given by $a_{ij}^{(z)} = 9(\delta_{iz}\delta_{jz} + \frac{1}{4}\delta_{ix}\delta_{jx} + \frac{1}{4}\delta_{iy}\delta_{jy})$ for z-type bonds (results for $\gamma = x, y$ follow from symmetry). We see that even rather small strain fields are sufficient to support s^y order locally: the new term becomes comparable with quadrupolar τ coupling already at $\delta \sim 1/3$. The sign of a_{ij} depends on the relative orientation of local distortions; for antiferro-type distortions ($\delta_i\delta_j < 0$), the s^y moments are coupled ferromagnetically, and vice versa (i.e., following Goodenough-Kanamori rules).

The lattice effects on the physical content of the E_g doublets should be essential for understanding the magnetic properties of $5d^2$ osmates. A qualitative picture is that while pseudospin one-half ordering in these compounds is predominantly of a quadrupolar type, there should also be a weak and spatially inhomogeneous dipolar component of the pseudospin order parameter, induced by the random distortions inevitable in real crystals.

VI. CONCLUSIONS

We have developed a microscopic theory for multipole orders in spin-orbit Mott insulators of non-Kramers d^2 ions, which have a nonmagnetic doublet ground state of E_g symmetry. The exchange Hamiltonians for dominant hopping processes are derived and expressed in terms of pseudospin-1/2 operators. Reflecting the spin-orbital mixed nature of the E_g wave functions, the pseudospin interactions are in general strongly anisotropic and depend on the bond directions. The phase behavior of these models on different lattices are considered by means of analytical and numerical methods.

On a honeycomb lattice, we find that interplay between direct overlap of t_{2g} orbitals and their hopping via ligand ions gives rise to a competition between two distinct multipole orders: vortex-type quadrupole order and collinear AF octupole order. These two states become degenerate at the parameter point where the model has a hidden SU(2) symmetry and is isomorphic to the FM Heisenberg model. The model also can be mapped to the extended Kitaev model for d^5 systems, which is useful to understand its global phase behavior.

On a triangular lattice, a combination of geometrical and spin-orbital frustrations result in a novel type of ordering, which can be viewed as a coherent superposition of vortex-type quadrupole and ferri-type octupole orders. This complex state appears as an intermediate phase between collinear AF and FM quadrupole states, as a compromise to their competition.

Double perovskite compounds of d^2 ions with strong SOC such as osmium Os^{6+} or rhenium Re^{5+} are discussed in more detail, including also Jahn-Teller coupling of electron quadrupole moments to lattice degrees of freedom. We find that the exchange and JT effects do work cooperatively to support quadrupole order in DP lattices. Static lattice distortions associated with this order are expected to be small, due to a reduction of the order parameters by the dynamical JT effect and pseudospin frustrations caused by bond-dependent interactions on the fcc lattice. Nevertheless, quadrupole order should lead to well detectable changes in phonon spectra as well as in nuclear magnetic resonance lineshapes. Signatures of JT dynamics in Raman and optical data should also be interesting to look for. A possible scenario for TR-symmetry breaking due to noncubic crystal fields near defects is suggested. We show that the local distortions modify the ground state wave functions, induce local magnetic moments and enhance their exchange interactions, illustrating the importance of the lattice effects for interpretation of the experimental data.

Overall, we have presented a theory for a class of pseudospin one-half systems based on non-Kramers $5d^2$ ions. The models introduced and discussed in this paper are of interest in their own right. From a materials perspective, our findings suggest rich physics yet to be explored in $5d^2$ spin-orbit Mott insulators with various lattice structures. Of special interest are the vortex-type states in honeycomb, and an unusual coherent mixture of quadrupole and octupole orders in triangular lattices. The present paper may form a theoretical basis for the future research of $5d^2$ ion compounds.

[1] J. B. Goodenough, *Magnetism and the Chemical Bond* (Interscience Publ., New York, 1963).

[2] K. I. Kugel and D. I. Khomskii, The Jahn-Teller effects and magnetism: Transition metal compounds, Sov. Phys. Usp. **25**, 231 (1982).

[3] G. Khaliullin, Orbital order and fluctuations in Mott insulators, Prog. Theor. Phys. Suppl. **160**, 155 (2005).

[4] T. Takayama, J. Chaloupka, A. Smerald, G. Khaliullin, and H. Takagi, Spin-orbit-entangled electronic phases in $4d$ and $5d$ transition-metal compounds, J. Phys. Soc. Jpn. **90**, 062001 (2021).

[5] We note that the notations E_g/e_g and T_{2g}/t_{2g} correspond to Γ_3 and Γ_5 representations of the cubic group, respectively.

[6] A. Abragam and B. Bleaney, *Electron Paramagnetic Resonance of Transition Ions* (Clarendon, Oxford, 1970).

[7] A. Takahashi and H. Shiba, Possible orbital orderings in a model of metallic double-exchange ferromagnets, J. Phys. Soc. Jpn. **69**, 3328 (2000).

[8] R. Maezono and N. Nagaosa, Complex orbital state in manganites, Phys. Rev. B **62**, 11576 (2000).

[9] J. van den Brink and D. I. Khomskii, Orbital ordering of complex orbitals in doped Mott insulators, Phys. Rev. B **63**, 140416(R) (2001).

[10] D. I. Khomskii, *Transition Metal Compounds* (Cambridge University Press, Cambridge, 2014).

[11] Y. Kuramoto, H. Kusunose, and A. Kiss, Multipole orders and fluctuations in strongly correlated electron systems, J. Phys. Soc. Jpn. **78**, 072001 (2009).

[12] D. D. Maharaj, G. Sala, M. B. Stone, E. Kermarrec, C. Ritter, F. Fauth, C. A. Marjerrison, J. E. Greedan, A. Paramekanti, and B. D. Gaulin, Octupolar Versus Néel Order in Cubic $5d^2$ Double Perovskites, Phys. Rev. Lett. **124**, 087206 (2020).

[13] C. M. Thompson, J. P. Carlo, R. Flacau, T. Aharen, I. A. Leahy, J. R. Pollichemi, T. J. S. Munsie, J. Munevar, T. Medina, S. Cheung, T. Goko, Y. J. Uemura, G. M. Luke, and J. E. Greedan, Long-range magnetic order in the $5d^2$ double perovskite Ba_2CaOsO_6: comparison with spin-disordered Ba_2YReO_6, J. Phys.: Condens. Matter **26**, 306003 (2014).

[14] C. A. Marjerrison, C. M. Thompson, A. Z. Sharma, A. M. Hallas, M. N. Wilson, T. J. S. Munsie, R. Flacau, C. R. Wiebe, B. D. Gaulin, G. M. Luke, and J. E. Greedan, Magnetic ground states in the three Os^{6+} $(5d^2)$ double perovskites Ba_2MOsO_6 ($M = $ Mg, Zn, and Cd) from Néel order to its suppression, Phys. Rev. B **94**, 134429 (2016).

[15] T. Aharen, J. E. Greedan, C. A. Bridges, A. A. Aczel, J. Rodriguez, G. MacDougall, G. M. Luke, V. K. Michaelis, S. Kroeker, C. R. Wiebe, H. Zhou, and L. M. D. Cranswick, Structure and magnetic properties of the $S = 1$ geometrically frustrated double perovskites La_2LiReO_6 and Ba_2YReO_6, Phys. Rev. B **81**, 064436 (2010).

[16] L. Lu, M. Song, W. Liu, A. P. Reyes, P. Kuhns, H. O. Lee, I. R. Fisher, and V. F. Mitrović, Magnetism and local symmetry breaking in a Mott insulator with strong spin orbit interactions, Nat. Commun. **8**, 14407 (2017).

[17] D. Hirai and Z. Hiroi, Successive symmetry breaking in a $J_{eff} = 3/2$ quartet in the spin-orbit coupled insulator Ba_2MgReO_6, J. Phys. Soc. Jpn. **88**, 064712 (2019).

[18] D. Hirai, H. Sagayama, S. Gao, H. Ohsumi, G. Chen, T. H. Arima, and Z. Hiroi, Detection of multipolar orders in the spin-orbit-coupled $5d$ Mott insulator Ba_2MgReO_6, Phys. Rev. Research **2**, 022063(R) (2020).

[19] D. Hirai and Z. Hiroi, Possible quadrupole order in tetragonal Ba_2CdReO_6 and chemical trend in the ground states of $5d^1$ double perovskites, J. Phys.: Condens. Matter **33**, 135603 (2021).

[20] G. Chen, R. Pereira, and L. Balents, Exotic phases induced by strong spin-orbit coupling in ordered double perovskites, Phys. Rev. B **82**, 174440 (2010).

[21] W. Witczak-Krempa, G. Chen, Y. B. Kim, and L. Balents, Correlated quantum phenomena in the strong spin-orbit regime, Annu. Rev. Condens. Matter Phys. **5**, 57 (2014).

[22] A. Paramekanti, D. D. Maharaj, and B. D. Gaulin, Octupolar order in d-orbital Mott insulators, Phys. Rev. B **101**, 054439 (2020).

[23] S. Voleti, D. D. Maharaj, B. D. Gaulin, G. Luke, and A. Paramekanti, Multipolar magnetism in d-orbital systems: Crystal field levels, octupolar order, and orbital loop currents, Phys. Rev. B **101**, 155118 (2020).

[24] G. Chen and L. Balents, Spin-orbit coupling in d^2 ordered double perovskites, Phys. Rev. B **84**, 094420 (2011).

[25] J. Kanamori, Crystal Distortion in Magnetic Compounds, J. Appl. Phys. **31**, S14 (1960).

[26] J. Chaloupka and G. Khaliullin, Highly frustrated magnetism in relativistic d^4 Mott insulators: Bosonic analog of the Kitaev honeycomb model, Phys. Rev. B **100**, 224413 (2019).

[27] J. Nasu, A. Nagano, M. Naka, and S. Ishihara, Doubly degenerate orbital system in honeycomb lattice: Implication of orbital state in layered iron oxide, Phys. Rev. B **78**, 024416 (2008).

[28] E. Zhao and W. V. Liu, Orbital Order in Mott Insulators of Spinless p-Band Fermions, Phys. Rev. Lett. **100**, 160403 (2008).

[29] C. Wu, Orbital Ordering and Frustration of p-Band Mott Insulators, Phys. Rev. Lett. **100**, 200406 (2008).

[30] C.-C. Chen, L. Muechler, R. Car, T. Neupert, and J. Maciejko, Fermionic Symmetry-Protected Topological Phase in a Two-Dimensional Hubbard Model, Phys. Rev. Lett. **117**, 096405 (2016).

[31] Z. Nussinov and J. van den Brink, Compass models: Theory and physical motivations, Rev. Mod. Phys. **87**, 1 (2015).

[32] G. Khaliullin, Order from disorder: Quantum spin gap in magnon spectra of $LaTiO_3$, Phys. Rev. B **64**, 212405 (2001).

[33] M. V. Mostovoy and D. I. Khomskii, Orbital Ordering in Frustrated Jahn-Teller Systems with $90°$ Exchange, Phys. Rev. Lett. **89**, 227203 (2002).

[34] K. Kubo, Quantum fluctuation induced order in an anisotropic pseudospin model, J. Phys. Soc. Jpn. **71**, 1308 (2002).

[35] G. Khaliullin, Excitonic Magnetism in Van Vleck-type d^4 Mott Insulators, Phys. Rev. Lett. **111**, 197201 (2013).

[36] J. H. Van Vleck, On the anisotropy of cubic ferromagnetic crystals, Phys. Rev. **52**, 1178 (1937).

[37] K. Kubo and T. Hotta, Influence of lattice structure on multipole interactions in Γ_3 non-Kramers doublet systems, Phys. Rev. B **95**, 054425 (2017).

[38] G. Jackeli and G. Khaliullin, Mott Insulators in the Strong Spin-Orbit Coupling Limit: From Heisenberg to a Quantum Compass and Kitaev Models, Phys. Rev. Lett. **102**, 017205 (2009).

[39] J. Chaloupka, G. Jackeli, and G. Khaliullin, Kitaev-Heisenberg Model on a Honeycomb Lattice: Possible Exotic Phases

in Iridium Oxides A_2IrO_3, Phys. Rev. Lett. **105**, 027204 (2010).

[40] J. Chaloupka and G. Khaliullin, Hidden symmetries of the extended Kitaev-Heisenberg model: Implications for the honeycomb-lattice iridates A_2IrO_3, Phys. Rev. B **92**, 024413 (2015).

[41] G. Khaliullin and S. Okamoto, Theory of orbital state and spin interactions in ferromagnetic titanates, Phys. Rev. B **68**, 205109 (2003).

[42] J. G. Rau, E. K.-H. Lee, and H.-Y. Kee, Generic Spin Model for the Honeycomb Iridates beyond the Kitaev Limit, Phys. Rev. Lett. **112**, 077204 (2014).

[43] I. Rousochatzakis, U. K. Rössler, J. van den Brink, and M. Daghofer, Kitaev anisotropy induces mesoscopic Z_2 vortex crystals in frustrated hexagonal antiferromagnets, Phys. Rev. B **93**, 104417 (2016).

[44] A. Catuneanu, J. G. Rau, H.-S. Kim, and H.-Y. Kee, Magnetic orders proximal to the Kitaev limit in frustrated triangular systems: Application to $Ba_3IrTi_2O_9$, Phys. Rev. B **92**, 165108 (2015).

[45] A. F. Albuquerque *et al.*, The ALPS project release 1.3: Open-source software for strongly correlated systems, J. Magn. Magn. Mater. **310**, 1187 (2007). Source codes of the libraries are available from http://alps.comp-phys.org/.

[46] B. Bauer, L. D. Carr, H. G. Evertz, A. Feiguin, J. Freire, S. Fuchs, L. Gamper, J. Gukelberger, E. Gull, S. Guertler

et al., The ALPS project release 2.0: open source software for strongly correlated systems, J. Stat. Mech. (2011) P05001.

[47] M. Troyer, B. Ammon, and E. Heeb, Parallel object oriented Monte Carlo simulations, Lect. Notes Comput. Sci. **1505**, 191 (1998).

[48] I. B. Bersuker, *The Jahn-Teller Effect* (Cambridge University Press, Cambridge, England, 2006).

[49] H. Liu and G. Khaliullin, Pseudo-Jahn-Teller Effect and Magnetoelastic Coupling in Spin-Orbit Mott Insulators, Phys. Rev. Lett. **122**, 057203 (2019).

[50] G. A. Gehring and K. A. Gehring, Co-operative Jahn-Teller effects, Rep. Prog. Phys. **38**, 1 (1975).

[51] N. Iwahara, V. Vieru, and L. F. Chibotaru, Spin-orbital-lattice entangled states in cubic d^1 double perovskites, Phys. Rev. B **98**, 075138 (2018).

[52] L. Xu, N. A. Bogdanov, A. Princep, P. Fulde, J. van den Brink, and L. Hozoi, Covalency and vibronic couplings make a nonmagnetic $j = 3/2$ ion magnetic, npj Quantum Mater. **1**, 16029 (2016).

[53] G. Jackeli and G. Khaliullin, Magnetically Hidden Order of Kramers Doublets in d^1 Systems: Sr_2VO_4, Phys. Rev. Lett. **103**, 067205 (2009).

[54] S. Guha and L. L. Chase, Vibronic and impurity-induced Raman scattering from a Jahn-Teller–distorted impurity, Phys. Rev. B **12**, 1658 (1975).